Biology of Reproduction, 2019, 101(4), 704–718
doi:10.1093/biolre/ioz113
Research Article
Advance Access Publication Date: 12 July 2019

Research Article

Auxin-inducible protein degradation as a novel approach for protein depletion and reverse genetic discoveries in mammalian oocytes†

Nicole J. Camlin and Janice P. Evans*

Department of Biochemistry and Molecular Biology, Bloomberg School of Public Health, Johns Hopkins University, Baltimore, Maryland, USA

***Correspondence:** Department of Biological Sciences, Purdue University, 915 W. State St., West Lafayette, IN 47907. Tel: +765-494-4407; Fax: (765) 496–1495; E-mail: janiceevans@purdue.edu

†**Grant support:** This work was funded by NIH grant HD087561 to JPE.
Conference presentation: Presented in part at the 51th Annual Meeting of the Society for the Study of Reproduction, July 10-13, 2018, New Orleans, Louisiana, USA.
Edited by Dr. Melissa E. Pepling

Received 6 January 2019; Revised 25 May 2019; Accepted 10 July 2019

Abstract

The disruption of protein expression is a major approach used for investigating protein function in mammalian oocytes. This is often achieved with RNAi/morpholino-mediated knockdown or gene knockout, leading to long-term loss of proteins of interest. However, these methods have noteworthy limitations, including (a) slow protein turnover can prohibit use of these approaches; (b) essential roles in early events precludes characterization of functions in subsequent events; (c) extended protein loss can allow time for compensatory mechanisms and other unanticipated events that confound interpretation of results. The work presented here examines the use of auxin-inducible degradation, a powerful new approach that overcomes these limitations through the depletion of one's protein of interest through controllable ubiquitin-mediated degradation. This method has been employed in yeast and mammalian cell lines, and here we demonstrate the utility of auxin-inducible degradation in mouse oocytes at multiple stages of meiosis, through degradation of exogenously expressed EGFP. We also evaluate important parameters for experimental design for use of this system in oocytes. This study thus expands the toolkit of researchers in oocyte biology, establishing the use of this unique and versatile approach for depleting proteins in oocytes, and providing researchers with valuable information to make use of this system.

Summary Sentence

Auxin-inducible degradation can be used to deplete proteins in oocytes throughout meiosis (prophase I to metaphase II), providing a valuable alternative to longer-term and post-transcriptional depletion methods such as knockdown and knockout.

Key words: auxin-inducible degradation, oocyte, meiosis, protein depletion.

Introduction

The disruption of protein expression is a major approach for investigating protein function for all cell types, including mammalian oocytes. Perturbation of a molecular target of interest can be achieved in a variety of ways, such as gene knockout and post-transcriptional knockdown, although with some potential challenges. One factor impacting RNAi- and morpholino-mediated knockdown and even conditional gene knockouts is protein half-life. A large proportion of proteins turn over in hours to days, but there are a number of proteins with half-lives ranging from months

to years [1]. RNAi/morpholino-mediated knockdown relies on culturing prophase I oocytes for 1–2 days to allow time for RNA degradation and/or translation suppression and protein turnover, and thus knockdown is completely dependent on a protein turning over in this 1–2 day time period. There are also extreme cases of proteins that cannot be depleted by conditional knockout, such as the histone-like centromeric protein CENP-A. *Gdf9-Cre*-driven conditional knockout, which inactivates floxed genes in oocytes beginning early in folliculogenesis, does not lead to obvious CENP-A protein loss, and instead, CENP-A is detected in oocytes from mice up to 14.5 months old [2].

Another challenge lies in the time constraints for the method of target depletion. Knockout approaches typically involve depleting the target of interest for the life of the organism/cell, or, for Cre-driven conditional knockouts, for the time when Cre recombinase is expressed from a given transcriptional driver. Post-transcriptional knockdown with RNAi or morpholinos can occur in shorter time frames, but knockdown still essentially depletes the target of interest for the remaining lifetime of the oocyte. This presents limitations to the analyses and discoveries that can be made. For example, if a protein is indispensable early in meiosis (e.g. meiosis I resumption), then its potential role at a later time point (e.g. metaphase I or egg activation upon fertilization) cannot be investigated.

Finally, another challenge with knockout and knockdown are unanticipated consequences that confound interpretation of results. The potential for off-target effects is one classic example of this. Another circumstance that can arise is the masking of a phenotype associated with compensatory effects, particularly if these compensatory effects develop over time with the long-term depletion of one's molecule of interest. Examples of this in oocyte biology include upregulation of cyclin B2 with oocyte-specific conditional knockout of cyclin B1, leading to partial rescue of meiosis [3], and upregulation of the Src family kinase Yes in oocytes from the Fyn knockout mouse, also likely ameliorating deleterious effects of loss of Fyn [4]. This and other unexpected effects of gene knockout may in part explain instances of disparate phenotypes revealed by different depletion approaches, with examples in oocyte biology being MASTL and BubR1 (also known as BUB1B) [5–10].

Perturbation of a target of interest can be done post-translationally as well. Small molecule inhibitors offer a way to impair protein function, with the advantage of readily allowing for temporal attenuation of protein activity, but the disadvantage of potential off-target effects. A recently developed approach for protein depletion, called Trim-Away, has been shown to remove proteins from mammalian oocytes at distinct stages of meiosis [11]. Trim-Away relies on microinjection of an antibody to the protein of interest, and thus is dependent on antibody availability and specificity [11]. Trim-Away also lacks straightforward temporal control as protein depletion begins immediately after antibody microinjection. A post-translational approach for temporally controllable and specific depletion of a protein of interest would be a highly valuable tool for research in oocyte biology, and we report here on such an approach, auxin-inducible degradation.

Auxin-inducible degradation is a powerful new approach that leverages inducible protein depletion. The auxin-inducible degradation system utilizes components of a cell's own ubiquitin-mediated protein degradation processes, along with a component taken from plants that is controlled by the plant hormone auxin. Part of this is the SCF E3 ubiquitin ligases, an evolutionarily conserved family of multimeric E3 ligases named for their subunits, SKP1, Cullin1 (CUL1), and F-Box protein. The F-Box protein dictates the substrate(s) of each SCF E3 ligase, and the auxin-inducible degradation system utilizes the plant-specific F-Box protein, TIR1 [12]. TIR1 can combine with endogenous SKP1 and CUL1 proteins in non-plant cells to form a functional E3 ubiquitin ligase [13–16]. Importantly, TIR1 only recognizes its degradation motif, auxin-inducible degron (AID), in the presence of auxin [17]. In cells expressing AID-tagged proteins and exogenous TIR1, addition of auxin leads to precisely timed and highly specific depletion of the AID-tagged target proteins (Figure 1A) [13–16]. In yeast and mammalian cultured cells, almost complete loss of AID-tagged proteins is observed in 30–90 min following auxin treatment [13, 15]. A very recent report used auxin-inducible degradation in metaphase II (MII)-arrested mouse eggs undergoing parthenogenetic activation in response to exogenously expressed phospholipase C ζ [18]. The work here examines the full utility of this system in mammalian oocytes using exogenously expressed AID-tagged EGFP. We evaluated crucial experimental variables for the use of the AID system in oocytes, including optimizing the system for live-cell imaging and testing the system at different stages of meiosis.

Materials and methods

Animals and ethics approval

CF-1 female mice (Envigo) aged 6–11 weeks were used in accordance with the Johns Hopkins University Animal Care and Use Committee guidelines. Mice were housed with ad libitum water and food under a 12 h light: dark cycle.

Plasmid constructs and cRNA synthesis

PCR with Phusion High-Fidelity DNA Polymerase (Thermo Fisher, F530S) was used to amplify cDNAs encoding AIDmini-EGFP and osTIR1–9myc (TIR1 from *Oryza sativa*; both parental plasmids were gifts from Andrew Holland, available from Addgene: AIDmini-EGFP [#101713], TIR1–9myc [#80073] [16]). Following gel purification, PCR products were digested with SalI (New England Biolabs (NEB), R0138S) and XbaI (NEB, R0145S), and cloned into pIVT/KAN2 (a gift from Carmen Williams) using the standard protocol. See Supplementary Table S1 for cloning primers and plasmid constructs. All plasmids were verified using DNA sequencing.

For cRNA synthesis, plasmids were linearized with NdeI (NEB, R0111S) and then purified with QIAquick Gel Extraction Kit (QIAGEN, 28704). In vitro transcription was performed with the mMESSAGE mMACHINE T7 or SP6 Transcription Kit (Thermo Fisher, AM1344 and AM1340) according to the manufacturer's instructions. Complementary RNA was resuspended in nuclease-free water at concentrations of 0.8–4.4 μg/μl.

Oocyte collection, microinjection, and in vitro maturation

Prophase I-arrested oocytes were collected in Whitten's-HEPES medium as previously described [19] (109.5 mM NaCl, 4.7 mM KCl, 1.2 mM KH_2PO_4, 1.2 mM $MgSO_4$, 5.5 mM glucose, 0.23 mM pyruvic acid, 4.8 mM lactic acid hemicalcium salt, with 7 mM $NaHCO_3$, 15 mM HEPES) supplemented with 0.25 μM milrinone (Sigma-Aldrich, M4659) to hold oocytes at prophase I arrest. For each injection experiment, oocytes were pooled from three to six females. Oocytes were transferred into Whitten's bicarbonate (Whitten's medium without HEPES and with 22 mM $NaHCO_3$ [19]) supplemented with milrinone. Prophase I oocytes were microinjected with cRNA into the cytoplasm (see the Results section

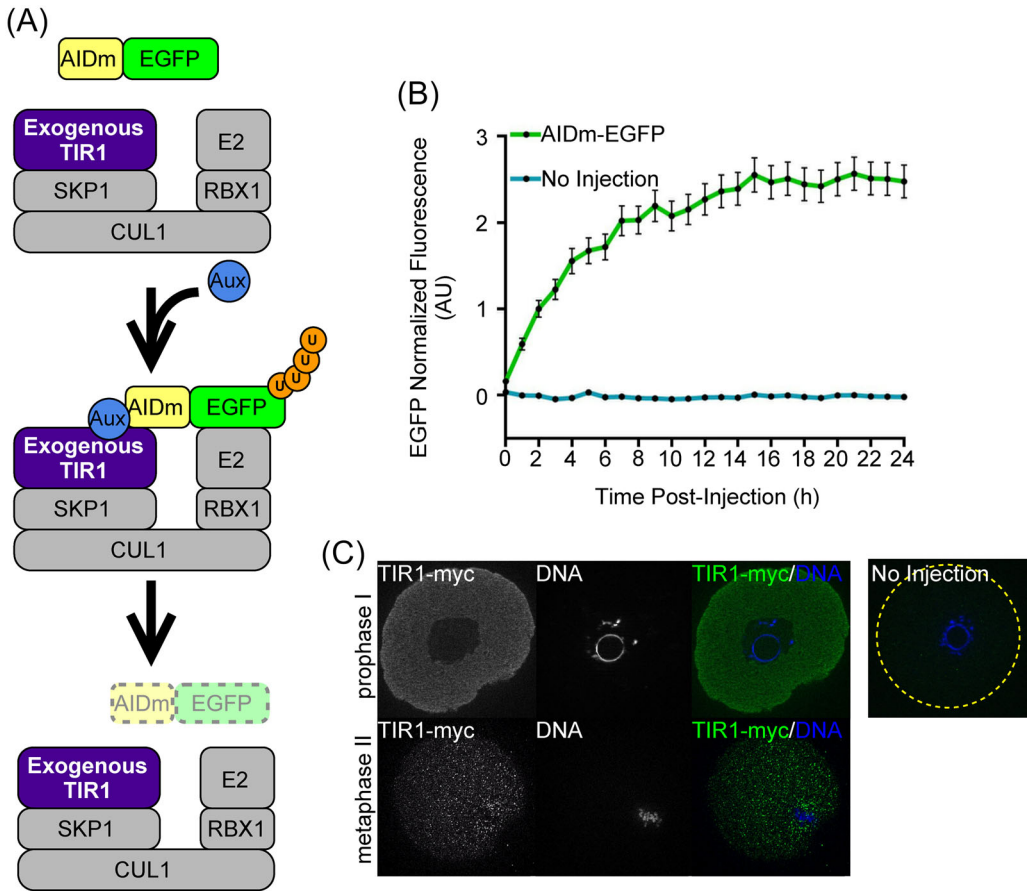

Figure 1. Overview of the auxin-inducible protein degradation system and exogenous expression of AIDm-EGFP and TIR1-myc in oocytes. (A) Schematic illustration of exogenously expressed TIR1 forming a functional SCF E3 ligase with endogenous SKP1 and CUL1 proteins. When cells are not exposed to auxin (Aux, blue circle), auxin-inducible degron (AIDm) tagged proteins are able to function normally. Addition of Aux leads to interaction of TIR1 with the AIDm, polyubiquitination (U, orange circles) of the AID-tagged protein, and ultimately proteasome-mediated degradation. (B) Graphical representation of EGFP fluorescence intensity over time in oocytes injected with 0.4 μg/μl AIDm-EGFP cRNA. EGFP fluorescence normalized to AIDm-EGFP expression at 2 h. (C) TIR1-myc immunofluorescence in prophase I and MII oocytes injected with 2.2 μg/μl TIR1 cRNA 16–18 h post-injection. Line graph shows mean and SEM of EGFP fluorescence every hour.

and figure legends for concentrations used; total concentrations of cRNA were 1–3 μg/μl) using a Nikon Eclipse TE 2000–5 microscope equipped with an Eppendorf FemtoJet. An injection pressure of 50–250 hPa and an injection time of 0.1–0.5 s were used. Oocytes were cultured in Whitten's bicarbonate or CZB medium (81.62 mM NaCl, 4.83 mM KCl, 1.18 mM KH_2PO_4, 1.18 mM $MgSO_4$, 25.12 7 mM $NaHCO_3$, 1.7 mM $CaCl_2$, 31.3 mM lactic acid hemicalcium salt, 0.27 mM pyruvic acid, 0.11 mM EDTA, 7 mM taurine, and 1 mM L-glutamine) supplemented with 0.25 μM milrinone at 37°C, 5% CO_2 for at least 3 h to allow for protein expression.

For in vitro maturation (IVM), prophase I oocytes were washed through CZB without milrinone. IVM occurred for 16 h at 37°C, 5% CO_2, either in a CO_2 incubator or on a Zeiss Axio Observer Z1 microscope equipped with a Zeiss Heating Unit XL S1, CO_2 Module S1, and Temp Module S1 (Carl Zeiss, Inc.). For experiments in which oocytes were cultured in a CO_2 incubator (i.e. in the dark) or cultured during live-cell imaging (i.e. exposed to light periodically), oocytes were exposed to auxin for the duration of IVM. Data from these experiments on maturation rates reflect the number of MII eggs resulting from the total number of oocytes subjected to IVM. On the other hand, in studies in which auxin was added to oocytes at 180 min into IVM, the reported maturation rates were the percentage of MII eggs resulting from number of oocytes that underwent germinal vesicle breakdown (GVBD) prior to auxin addition. Meiosis I timing was calculated as the difference between GVBD and polar body emission.

Live-cell imaging and image analysis

Oocytes were cultured in CZB medium droplets under mineral oil (Sigma-Aldrich, M3516) in glass bottom culture dishes (MatTek, P35G-0-14-C). For all experiments using prophase I-arrested oocytes, culture media were supplemented with 0.25 μM milrinone. Oocytes were incubated at 37°C, 5% CO_2 with images taken every 20 min or 180 min for the duration of the experiment on a Zeiss Axio Observer Z1 microscope with AxioCam MRm Rev3 camera (Carl Zeiss, Inc.). For degradation studies, auxin, cycloheximide (CHX; Millipore Sigma, 239764; dissolved in ethanol), or auxin with CHX were added to the culture droplets at the indicated time points, to final concentrations of 500, 1000, or 2000 μM auxin and 10 μg/ml CHX. Naturally occurring auxin, 3-indoleacetic acid (IAA; Sigma-Aldrich, I5148; dissolved in H_2O), and synthetic auxin, 1-naphthaleneacetic acid (NAA; Sigma-Aldrich, N0640; dissolved in 1N NaOH) were used, with auxin type indicated for each experiment. Following auxin/CHX addition, imaging continued

every 20 min. For experiments using 1000 to 2000 μM IAA, images were only taken four times, prior to IAA addition (t = −20 min) and 180, 360, and 520 min post-IAA addition. For recovery studies, after microinjection oocytes were held arrested in CZB supplemented with 0.25 μM milrinone and vehicle, 500 μM IAA, or 500 μM NAA for 16 h. Oocytes were then washed into CZB with milrinone and vehicle, 500 μM IAA, or 500 μM NAA and imaged every 20 min for 8 h.

ImageJ Fiji distribution (Freeware; National Institutes of Health—https://imagej.nih.gov/ij/[20]) was used to measure the EGFP fluorescence intensity for each oocyte, taking into account background fluorescence and oocyte area as previously described [21]. For degradation experiments, the fluorescence intensity of each oocyte was normalized in order to account for oocyte-to-oocyte variability in starting EGFP fluorescence, by setting a value of 1 for the fluorescence intensity detected at time point t = −180 min or t = −20 min. For examination of GVBD, only oocytes that underwent GVBD within 3 h of milrinone washout (i.e. those that appeared to be meiotically competent) were included in the analysis. For recovery experiments, fluorescence intensity was normalized in two different ways: (1) EGFP fluorescence intensity at t = 20 min was set to 1 for each oocyte; or (2) the average fluorescence intensity of vehicle control group at t = 20 min was set to a value of 1, and this was used to normalize all other groups.

AIDm-EGFP half-life was calculated using GraphPad Prism 7 software (GraphPad Software). The AIDm-EGFP fluorescence intensity over time for oocytes microinjected with 2–2.2 μg/μl TIR1 and exposed to 500 μM auxin was pooled based on stage of meiosis (prophase I, GVBD, and MII) or auxin type (IAA at GVBD, or NAA at GVBD). Data were normalized such that t = −20 min equaled 1, and oocytes that had an EGFP fluorescence intensity greater than 1 at 480 min (prophase I and GVBD) or 180 min (MII) were excluded. Non-linear (one-phase) regression analysis with least squares (ordinary) fit was performed on the average EGFP fluorescence intensity over time.

Immunofluorescence

Zona pellucida removal was performed by incubating oocytes briefly in acidic MEM-compatible medium (116.4 mM NaCl, 5.4 mM KCl, 10 mM HEPES, 1 mM NaH_2PO_4, 0.8 mM $MgSO_4$, pH 1.5). Oocytes were then fixed in 4% paraformaldehyde (Sigma-Aldrich, P6148) in PBS at room temperature for 30 min, permeabilized in PBS with 0.1% Triton X-100 (Fisher Scientific, BP151–500) for 15 min at room temperature, and blocked in PBS with 0.1% BSA (Sigma-Aldrich, A9647) and 0.01% Tween-20 (Sigma-Aldrich, P7949) for 1 h at room temperature. Anti-Myc primary antibody (Thermo Fisher, MA1–21316) was used at a final concentration of 4 μg/ml. After overnight incubation with anti-Myc antibody, oocytes were washed three times in PBS with 0.1% BSA and 0.1% Tween-20 before incubation with 7.5 μg/ml goat anti-mouse IgG conjugated to Alexa Fluor 488 (Jackson ImmunoResearch) for 1 h at room temperature. Following three washes in PBS with 0.1% BSA and 0.1% Tween-20, oocytes were mounted in VectaShield containing 0.75 μg/ml 4′-6′-diamidino-2-phenylindole (DAPI; Sigma-Aldrich, D9542). Imaging was performed using a Zeiss Axio Observer Z1 microscope with AxioCam MRm Rev3 camera and ApoTome optical sectioning (Carl Zeiss, Inc.).

Statistics

GraphPad Prism 7.0 software was used for statistical analysis. For categorical data, the Fisher's exact test was used. Numerical data were tested for normal distribution using the D'Agnostino–Pearson omnibus normality test. For data that followed a normal distribution, ANOVA with Tukey's post hoc test was used. For all other data, Kruskal–Wallis test with Dunn's post hoc or Mann–Whitney test was used. A P-value < 0.05 was considered statistically significant. Further information on statistics tests used for each dataset can be found within the figure legends.

Results

Exogenous expression of AIDm-EGFP and TIR1-myc in oocytes

As part of our first evaluation of auxin-inducible degradation in oocytes, we verified expression of our test substrate, AIDm-EGFP, and of a myc-tagged version of the F-box protein TIR1 from the rice *O. sativa* (TIR1-myc). Prophase I oocytes were microinjected with cRNA encoding AIDm-EGFP (0.4 μg/μl) and live imaged for EGFP fluorescence over a course of 24 h (Figure 1B). Exogenous expression of AIDm-EGFP increased gradually over time, when compared to uninjected control oocytes, and EGFP fluorescence accumulated sufficiently over 3–6 h such that EGFP fluorescence loss could be characterized in further experiments. TIR1-myc cRNA (2.2 μg/μl) was also injected into prophase I oocytes, and then immunofluorescence analysis with an anti-Myc antibody was performed on oocytes that were held arrested at prophase I for 18 h or were in vitro matured to metaphase II for 16 h. This analysis showed that TIR1-myc-cRNA-injected oocytes express TIR1-myc, with TIR1-myc signal observed throughout the cytoplasm (Figure 1C).

Extent of auxin-inducible degradation in prophase I oocytes is dependent on the amount of TIR1

We next sought to determine if auxin-inducible degradation could occur in oocytes, and what concentration TIR1-myc cRNA was needed to induce degradation. Prophase I oocytes were microinjected with cRNA encoding AIDm-EGFP (0.4 μg/μl) and decreasing concentrations of TIR1-myc cRNA (2.2–0.5 μg/μl). Oocytes were cultured for 3 h prior to imaging to allow time for translation of exogenous AIDm-EGFP and TIR1-myc from the injected cRNA. One hundred and eighty minutes after imaging began (6 h post-injection), 500 μM IAA (a naturally occurring auxin) was added to culture. A reduction in AIDm-EGFP fluorescence was observed in all IAA-exposed oocytes injected with TIR1-encoding cRNA (Figure 2A and B). Comparison of fluorescence intensity 20 min prior to IAA addition (noted as "−20 min" hereafter) and 180 min after IAA addition revealed a significant reduction in AIDm-EGFP in all IAA-exposed oocytes, which was not observed in vehicle-only controls (Figure 2C; 2.2 μg/μl TIR1 cRNA, 30.7 ± 2.3% AIDm-EGFP loss, $P \leq 0.0001$; 1.1 μg/μl TIR1 cRNA, 23.8 ± 2.0% AIDm-EGFP loss, $P \leq 0.0001$; 0.5 μg/μl TIR1 cRNA, 17.4 ± 2.3% EGFP loss, $P \leq 0.0001$). This decrease in AIDm-EGFP was found to be dose-dependent, with 2.2 and 1.1 μg/μl TIR1-myc cRNA leading to significantly more loss of AIDm-EGFP fluorescence than 0.5 μg/μl (Figure 2C; 2.2 μg/μl vs. 0.5 μg/μl, $P \leq 0.0001$; 1.1 μg/μl vs. 0.5 μg/μl, $P = 0.0391$). Moving forward, we used 2.2 μg/μl of TIR1-myc cRNA, as it led to the most robust AIDm-EGFP loss in these studies.

Extended culture time and inhibition of translation does not enhance loss of exogenously expressed AIDm-EGFP with auxin-induced degradation

Having established that the extent of auxin-inducible degradation was dependent on the dose of TIR1-myc cRNA injected, we next

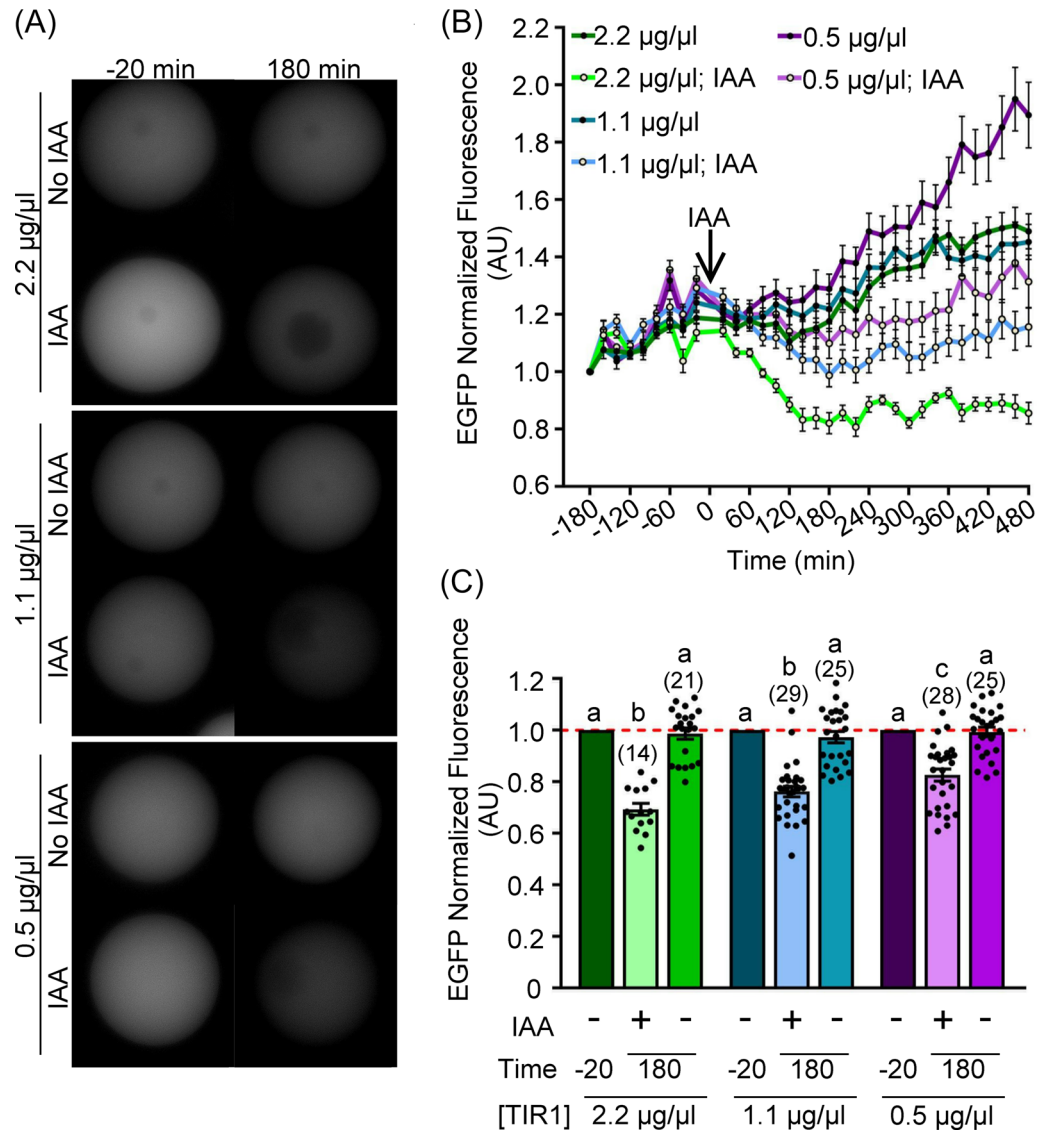

Figure 2. Range of TIR1-myc cRNA concentrations allows for depletion of exogenously expressed AIDm-EGFP. Prophase I oocytes were microinjected with 0.4 μg/μl AIDm-EGFP and 2.2, 1.1, or 0.5 μg/μl TIR1 cRNA 6 h prior to 500 μM IAA treatment. (A) Live-cell EGFP fluorescence (gray) in prophase I oocytes 20 min prior to (−20 min) and 180 min after IAA addition. (B) Graphical representation of EGFP fluorescence over time. 500 μM IAA was added at 0 min (arrow). EGFP fluorescence normalized to expression at −180 min. (C) Graphical comparison of EGFP fluorescence before (−20 min) and after (180 min) IAA addition. EGFP fluorescence was normalized to expression at −20 min (ANOVA with Tukey's post hoc). n = number of oocytes analyzed (15–29 over 2–3 technical replicates), $P \leq 0.0391$. Line graph shows mean and SEM of EGFP fluorescence every 20 min. Bar graph shows mean, SEM, and individual oocyte scatter plot.

examined if time of exogenous expression of AIDm-EGFP and TIR1 following cRNA injection would influence AIDm-EGFP loss. In these experiments, oocytes were allowed 16 h prior to live-cell imaging and IAA addition to translate AIDm-EGFP and TIR1-myc from the injected cRNA, increasing the post-injection culture time from the 6 h used in the experiments noted above. Over a period of 3 h of live-cell imaging, during which oocytes were treated with 500 μM IAA or vehicle, a reduction in exogenous AIDm-EGFP fluorescence was observed over time in both groups, but was more pronounced in the IAA group (Figure 3A). Analysis of fluorescence intensity just prior to (t = −20 min) IAA addition and at 180 min after IAA addition revealed that this reduction was statistically significant for both IAA-treated and vehicle-only control oocytes (Figure 3B; IAA, 29.5 ± 0.9% AIDm-EGFP loss, $P \leq 0.0001$; vehicle, 5.2 ± 0.8%, $P \leq 0.0001$). Addition of auxin at 0 min led to an increase in AIDm-EGFP loss when compared to vehicle-only oocytes (IAA vs. vehicle, $P \leq 0.0001$). Taken together, these results showed that allowing 16 h for protein expression after cRNA injection led to comparable auxin-inducible AIDm-EGFP degradation as observed with 6 h (30.7% loss with 6 h culture after cRNA injection (Figure 2C) vs. 29.5% with 16 h culture after cRNA injection (Figure 3B)).

We observed that EGFP fluorescence intensity never dropped below 0.7 arbitrary units (AU) by 180 min post-IAA treatment. To determine what effect continued translation of exogenous AIDm-EGFP cRNA had on EGFP loss, we treated prophase I oocytes with the translation inhibitor cycloheximide (CHX), either alone or in combination with 500 μM IAA; oocytes treated with 500 μM IAA only were another experimental group. As expected, addition of

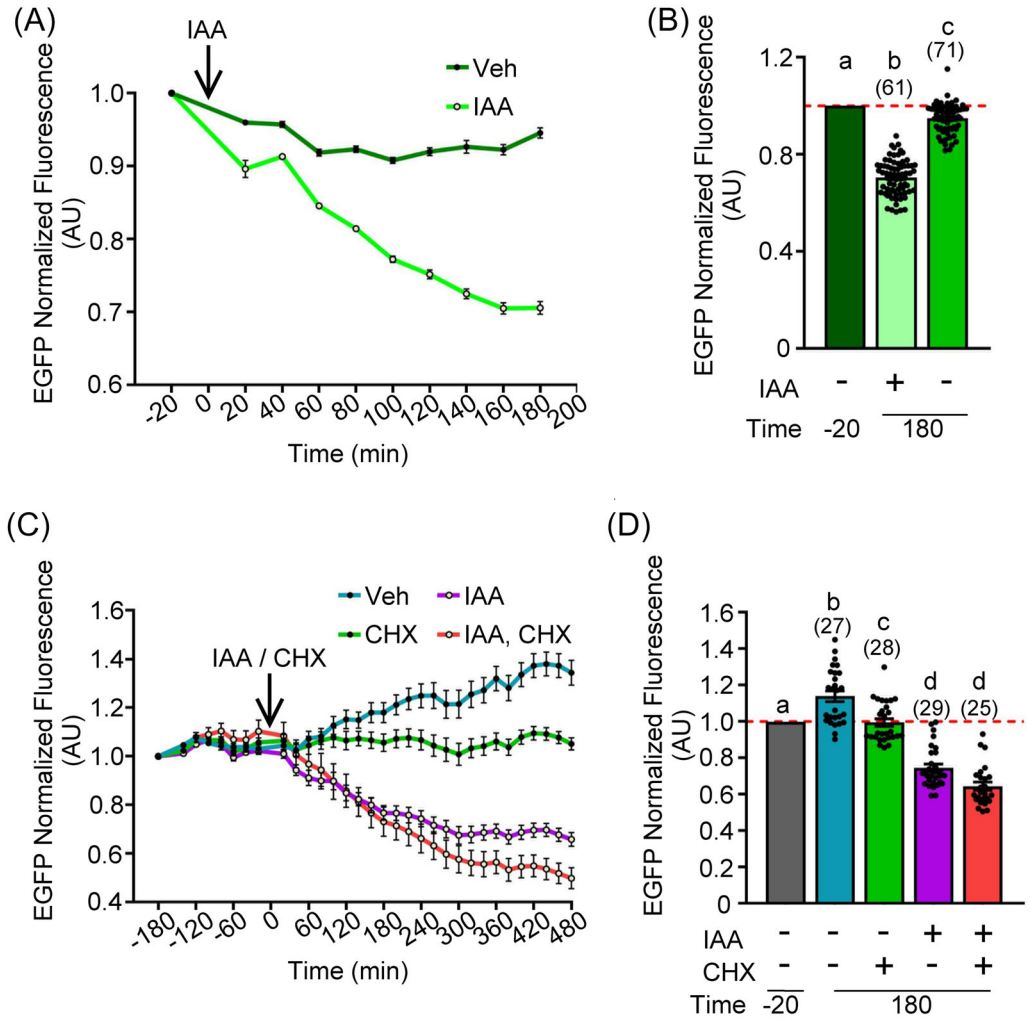

Figure 3. Increasing cRNA expression time or inhibiting translation with cycloheximide has no impact on loss of exogenously expressed AIDm-EGFP. (A, B) Oocytes were injected with 0.4 μg/μl AIDm-EGFP cRNA and 2.0–2.2 μg/μl TIR1-myc cRNA, and allowed to express cRNA for 16 h prior to 500 μM IAA treatment. (A) Graphical representation of EGFP fluorescence over time. 500 μM IAA was added at 0 min (arrow). EGFP fluorescence normalized to expression at −20 min. (B) Graphical comparison of EGFP fluorescence before (−20 min) and after (180 min) IAA addition. EGFP fluorescence was normalized to expression at −20 min (ANOVA with Tukey's post hoc). n = number of oocytes analyzed (61–71 over two technical replicates), $P < 0.0001$. (C, D) Oocytes were injected with 0.4 μg/μl AIDm-EGFP cRNA and 2.0 μg/μl TIR1-myc cRNA, and allowed to translate protein from the injected cRNA for 6 h prior to 500 μM IAA and/or CHX treatment. (C) Graphical representation of EGFP fluorescence over time. IAA and/or CHX were added at 0 min (arrow). EGFP fluorescence normalized to expression at −180 min. (D) Graphical comparison of EGFP fluorescence before (−20 min) and after (180 min) IAA and/or CHX addition. EGFP fluorescence normalized to expression at −20 min (Kruskal–Wallis test with Dunn's post hoc). n = number of oocytes analyzed (25–29 over two technical replicates), $P \leq 0.0072$. Line graphs show mean and SEM of EGFP fluorescence every 20 min. Bar graphs show mean, SEM, and individual oocyte scatter plots.

CHX prevented further EGFP accumulation (Figure 3C). The combination of IAA + CHX resulted in a further decrease in EGFP fluorescence as compared to IAA, but only at 480 min post-IAA exposure (Figure 3C; 0.66 ± 0.03 (IAA) vs. 0.50 ± 0.04 (IAA + CHX) AU) and not 180 min post-IAA exposure. Analysis of EGFP fluorescence intensity at 180 min following IAA/IAA + CHX addition revealed no significant decrease between oocytes treated with IAA and oocytes treated with IAA + CHX (Figure 3D; 0.75 ± 0.02 [IAA] vs. 0.64 ± 0.02 [IAA + CHX], $P > 0.9999$). Data analysis for these experiments was performed in two different ways: (a) measurement of oocyte fluorescence intensity adjusted to field background (the area outside the oocyte) and oocyte area prior to normalization of −180 min (Figure 3C) or −20 min (Figure 3D) to 1; or (b) subtraction of fluorescence intensity of *uninjected* oocytes prior to normalization. This second method of normalization decreased final EGFP fluorescence at 480 min by a further 20% in IAA-exposed oocytes (Supplementary Figure S1; IAA, 0.39 ± 0.02 AU; IAA + CHX, 0.20 ± 0.03 AU). This suggests that oocyte autofluorescence and continued AIDm-EGFP cRNA translation contribute to the fluorescence signal detected. As such, an EGFP fluorescence intensity value of ∼0.6 AU equates to almost complete EGFP loss.

Auxin-inducible degradation occurs in oocytes during meiosis I and at metaphase II

The ability to perform precise and temporally controlled depletion of proteins at distinct points of meiosis is a key motivation for establishing use of auxin-inducible degradation in oocytes. Having

optimized conditions for auxin-inducible degradation in prophase I oocytes, we next ascertained if auxin-inducible protein degradation could be utilized at other stages of oocyte meiosis, namely after oocytes had resumed meiosis (GVBD), and at metaphase II (MII) arrest. In these experiments, prophase I-arrested oocytes were microinjected with AIDm-EGFP and TIR1-myc cRNAs. For analyses of GVBD oocytes, oocytes were washed out of milrinone-supplemented medium 180 min prior to IAA treatment; only oocytes that underwent GVBD before IAA exposure were included in analyses. For MII oocytes, oocytes injected at prophase I were subjected to IVM for 16 h, and treated with IAA at metaphase II arrest. A significant reduction in EGFP signal was observed between vehicle-only control and 500 μM IAA-treated oocytes at each of these stages of meiosis (Figure 4A–D; prophase I, 20.3 ± 3.1% AIDm-EGFP loss, $P \leq 0.0001$; GVBD, 28.3 ± 3.8% AIDm-EGFP loss, $P \leq 0.0001$; MII, 49.8 ± 2.3% AIDm-EGFP loss, $P \leq 0.0001$). Comparison of exogenous AIDm-EGFP fluorescence before (t = −20 min) and after (t = 180 min) IAA addition showed similar extents of EGFP loss in oocytes at these three stages of meiosis. However, no IAA-treated GVBD oocytes progressed through meiosis to produce first polar bodies during these live-cell imaging experiments. This failure to complete meiosis I was not observed in vehicle-only control oocytes (data not shown), suggesting a deleterious effect of IAA and/or auxin-inducible degradation on completion of meiotic maturation.

Comparison of IAA and NAA for live-cell imaging experiments

We next sought to determine the cause of the meiotic failure observed during live-cell imaging in IAA-treated oocytes exogenously expressing AIDm-EGFP and TIR1-myc. In yeast, exposure to IAA during live-cell imaging suppressed cell proliferation, and this impaired cell proliferation was not observed with the synthetic auxin NAA [22]. This growth defect was speculated to be caused by free radicals and nucleophiles accumulating as a result of IAA photodegradation, which occurs at UV to blue wavelengths [22–24]. To test whether the oocytes' failure to complete meiotic maturation could be associated with IAA photodegradation, oocytes were subjected to IVM, in the presence of 500 μM IAA or NAA, in the dark (i.e. in a CO_2 incubator) or during live-cell imaging with white light and 470 nm wavelength light, as performed in studies noted above (Figures 2–4). Vehicle-only control and NAA-treated oocytes progressed through first polar body emission in both culture conditions (Figure 5A and B; percentages of oocytes that emitted first polar bodies, vehicle-treated, 85.7% in dark, 62.9% during imaging, $P = 0.0539$; NAA-treated, 80.0% in dark, 84.1% during imaging, $P = 0.7769$). In contrast, IAA-treated oocytes only completed meiosis I in the dark. The extent of meiosis I completion of IAA-treated oocytes in the dark was comparable to vehicle-treated and NAA-treated oocytes, whereas exposure of IAA-treated oocytes to live-cell imaging conditions completely prevented meiotic maturation, as measured by first polar body emission (Figure 5A and B; IAA, 73.8% in dark vs. 0.0% during imaging; $P \leq 0.0001$). Of note, in plant cell culture medium this IAA photodegradation can be eliminated with yellow long-pass filters that remove UV, violet, and blue wavelengths [23]. Therefore, we next sought to determine if IAA-treated oocytes could complete meiosis when exposed to 556 nm (green wavelength) or 640 nm (red wavelength) excitation every 20 min during IVM. Excitation of IAA-treated oocytes at 556 nm significantly impacted their ability to complete meiosis I and emit the first polar body (Figure 5C; 91.8% (Veh) vs. 51.1% (IAA); $P < 0.0001$). In contrast, excitation at 640 nm had no effect on maturation of IAA-exposed oocytes (Figure 5C; 90.0% (Veh) vs. 80.5% (IAA); $P = 0.3493$).

Given that NAA did not appear toxic to completion of meiotic maturation during live-cell imaging with white light and wavelength 470 nm, we evaluated if NAA could induce exogenous AIDm-EGFP loss. Prophase I oocytes were microinjected with cRNAs encoding exogenous AIDm-EGFP and TIR1-myc as described above. After 180 min of expression, oocytes were subjected to IVM and imaged for 180 min prior to auxin addition (500 μM IAA or NAA). IAA and NAA led to comparable extents of EGFP loss, and EGFP loss was not observed in vehicle-only controls (Figure 6A and B; 34.1 ± 1.4% [IAA] vs. 30.1 ± 1.6% [NAA] EGFP loss; $P > 0.9999$). Importantly, NAA-treated oocytes were able to complete meiosis I, with extents of first polar body emission comparable to vehicle-only control oocytes (Figure 6D; 76.8% (vehicle) vs. 73.9% (NAA) MII eggs; $P = 0.8186$). Meiosis I timing, measured as the time from GVBD to first polar body emission, was also comparable between NAA-treated oocytes and vehicle-only control oocytes (Figure 6E; 646.4 ± 10.0 min (vehicle) vs. 643.5 ± 12.3 min (NAA); $P = 0.6655$).

Half-life of exogenously expressed AIDm-EGFP varies by meiotic stage but not auxin type

A key feature of auxin-inducible degradation is the ability to rapidly deplete proteins, with complete protein loss in mammalian cell lines occurring in 30–90 min, with a half-life ($t_{1/2}$) of AID-tagged proteins of 10–50 min [13, 15, 25–28]. The $t_{1/2}$ times of exogenous AIDm-EGFP in 500 μM IAA-treated prophase I, GVBD, and MII oocytes injected with 2–2.2 $\mu g/\mu l$ TIR1-myc cRNA were 106.9, 82.4, and 41.0 min, respectively. The differences in $t_{1/2}$ time between stage of meiosis were statistically significant ($P < 0.0001$). Treatment of GVBD oocytes with 500 μM NAA resulted in an AIDm-EGFP $t_{1/2}$ of 65.1 min, which was not different from the $t_{1/2}$ of AIDm-EGFP in IAA-treated GVBD oocytes ($P = 0.4275$).

Increasing auxin concentration has no impact on auxin-inducible degradation

We observed that exogenously expressed AIDm-EGFP in prophase I and GVBD oocytes had a half-life of ~2- to 11-fold greater than the protein half-life observed in mammalian mitotic cell lines [13, 15, 25–28]. As mouse oocytes are ~4 times larger than mitotic cells, we wondered if this could be a consequence of a decreased auxin gradient within the cell. Therefore, we examined the effects of higher auxin concentrations in the culture medium on auxin-inducible degradation. Complementary RNAs encoding AIDm-EGFP and TIR1-myc were microinjected into prophase I oocytes. Live-cell imaging began 180 min post-injection. Addition of NAA (500 and 1000 μM) at t = 0 min led to a significant reduction in EGFP fluorescence at t = 180 min when compared to vehicle-only treated oocytes (Figure 7A and B; $P < 0.0001$). Increasing NAA concentration to 1000 μM had no impact on EGFP loss at t = 180 min (Figure 7B; 40.0 ± 1.5% (500 μM NAA) vs. 33.1 ± 1.8% (1000 μM NAA) EGFP loss; $P > 0.9999$). NAA at concentrations higher than 1000 μM were not tested to minimize the amount of solvent, 1N NaOH, in culture medium. Similar studies were performed with IAA. Due to the toxicity of light-induced degradation of IAA, we tested increased IAA concentrations under altered imaging conditions, reducing light exposure by imaging every 180 min for 540 min (Figure 7C). Addition of IAA led to a reduction in EGFP fluorescence over time when compared to vehicle-treated oocytes (Figure 7D; $P < 0.0001$). However, as with NAA, increasing the

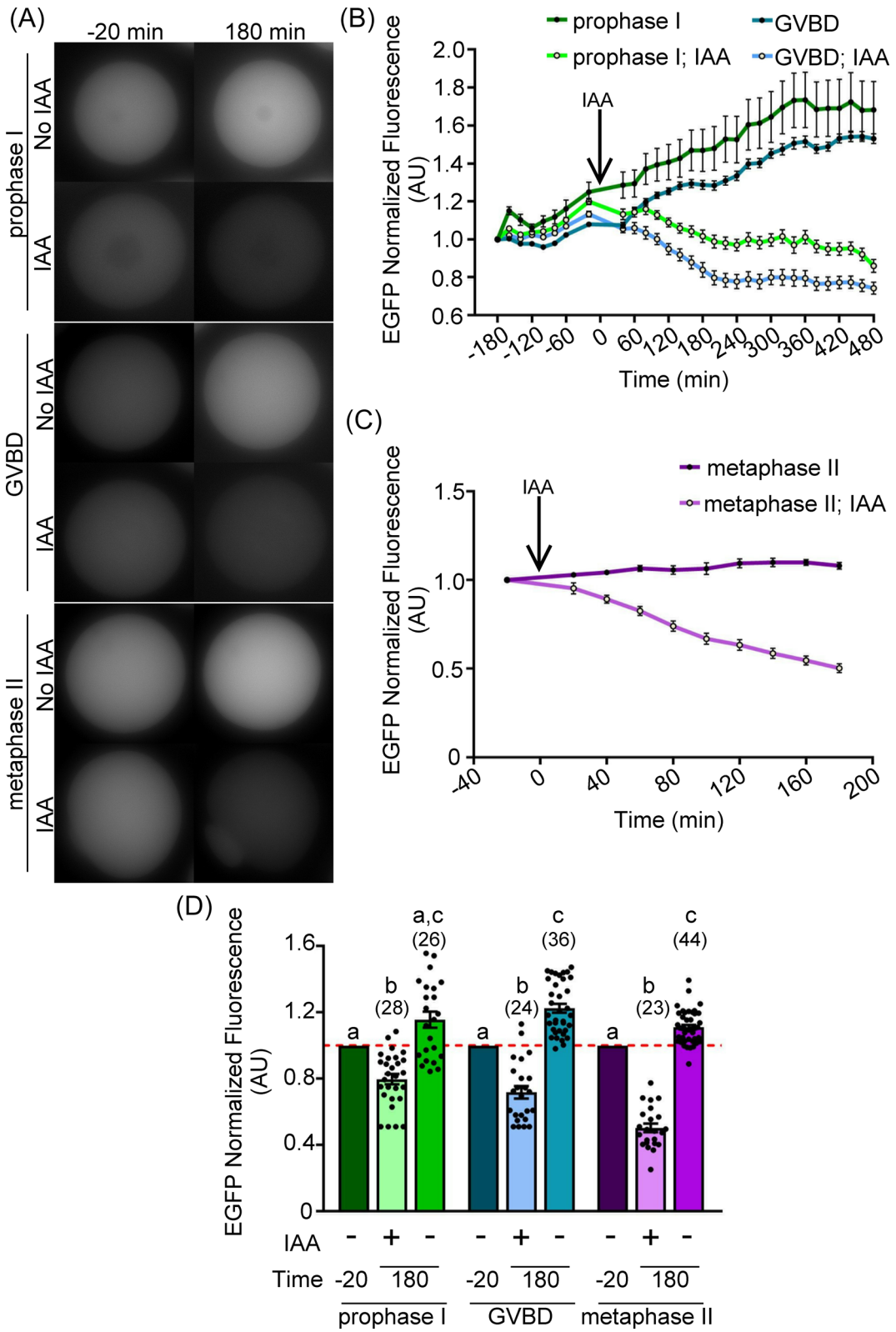

Figure 4. Auxin-inducible degradation works during meiosis I and at metaphase II (MII) arrest. Oocytes were injected with 0.4 μg/μl AIDm-EGFP cRNA and 2.0–2.2 μg/μl TIR1-myc cRNA, and allowed to express cRNA for 3 h prior to imaging and initiation of meiotic maturation (GVBD oocytes). (A) Live-cell EGFP fluorescence (gray) in oocytes 20 min prior to (−20 min) and 180 min after IAA addition. (B, C) Graphical representation of EGFP fluorescence over time in prophase I, GVBD (B), or MII (C) oocytes. IAA was added at a concentration of 500 μM at t = 0 min (arrow). EGFP fluorescence normalized to expression at −180 min (prophase I and GVBD) or −20 min (MII). (D) Graphical comparison of EGFP fluorescence before (−20 min) and after (180 min) IAA addition. EGFP fluorescence normalized to expression at −20 min (Kruskal–Wallis test with Dunn's post hoc). n = number of oocytes analyzed (23–44 over three technical replicates), $P < 0.0001$. Line graphs show mean and SEM of EGFP fluorescence every 20 min. Bar graph shows mean, SEM, and individual oocyte scatter plot.

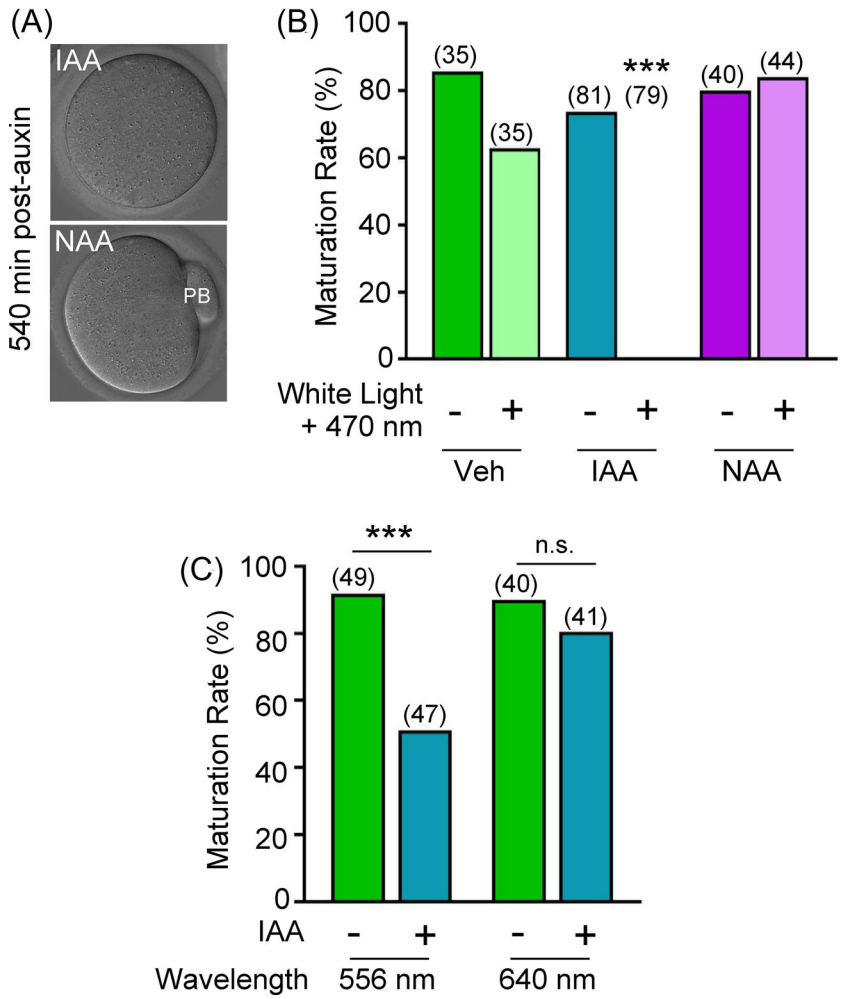

Figure 5. Auxin type impacts meiotic maturation with live-cell imaging. Impact of exposure to light and/or auxin (IAA or NAA) on oocyte maturation rate. (A) DIC images of oocytes at 540 min post-milrinone washout. Oocytes were exposed to white light + 470 nm wavelength light every 20 min, and 500 μM IAA or NAA throughout in vitro maturation (IVM). (B) Graphical representation of percentage of oocytes at MII following 16 h of IVM in vehicle, 500 μM IAA, or 500 μM NAA with (+) or without (–) exposure every 20 min to white light and 470 nm wavelength light. n = number of oocytes analyzed (35–79 over three technical replicates), $^{***}P \leq 0.0001$. (C) Graphical representation of percentage of oocytes at MII following 16 h IVM in vehicle or 500 μM IAA with exposure every 20 min at 556 or 640 nm wavelength light. n = number of oocytes analyzed (40–49 over three technical replicates), $^{***}P \leq 0.0001$. Bar graphs show percentage of oocytes that emitted a first polar body (PB).

concentration of IAA had no impact on the extent of EGFP loss at t = 180 min (Figure 7D; 40.1 ± 2.5% (500 μM IAA) vs. 28.4 ± 4.4% (1000 μM IAA) vs. 22.9 ± 4.4% (2000 μM IAA) EGFP loss; $P > 0.9999$ (500 μM vs. 1000 μM) and 0.3581 (500 μM vs. 2000 μM)).

Removal of auxin allows for recovery of exogenous AIDm-EGFP expression

Having examined the time frame of degradation of an exogenous protein (AIDm-EGFP) in an auxin-inducible-dependent manner, we wanted to determine if levels of this protein would recover after auxin removal. Prophase I oocytes were injected with cRNAs encoding TIR1-myc and AIDm-EGFP, and then subjected to 16 h of incubation in medium with vehicle, 500 μM NAA, or 500 μM IAA (treatment 1). Following this 16 h incubation, oocytes were washed into medium containing vehicle, 500 μM NAA, or 500 μM IAA (treatment 2), and live-cell imaged. Due to oocyte-to-oocyte variability in starting EGFP fluorescence, statistical analysis was performed with EGFP fluorescence at t = 20 min set to a value 1 for all oocytes (Figure 8A). The trends observed from this normalization are in agreement with those observed when oocyte EGFP fluorescence intensity was normalized to the average of vehicle-only exposed oocytes at t = 20 min (Figures 8B, Supplementary Figure S2A). There was no change in EGFP fluorescence in oocytes treated with vehicle throughout the duration of the experiment, i.e. in treatments 1 and 2 (Figure 8A; $P > 0.9999$). In oocytes incubated in vehicle for treatment 1 then exposed to IAA in treatment 2, there was a significant reduction in EGFP fluorescence when comparing t = 20 min to t = 500 min, indicating a continued sensitivity of the system to auxin (Figure 8A; 46.6 ± 2.4% EGFP loss; $P < 0.0001$). With regard to the ability of levels of AIDm-EGFP to recover, this was different between oocytes initially treated with NAA vs. IAA. After removal of NAA (i.e. exposure to NAA in treatment 1, then transfer to vehicle for treatment 2), EGFP fluorescence showed an 83.2 ± 1.1% increase by 500 min (Figure 8A; $P < 0.0001$), which was not

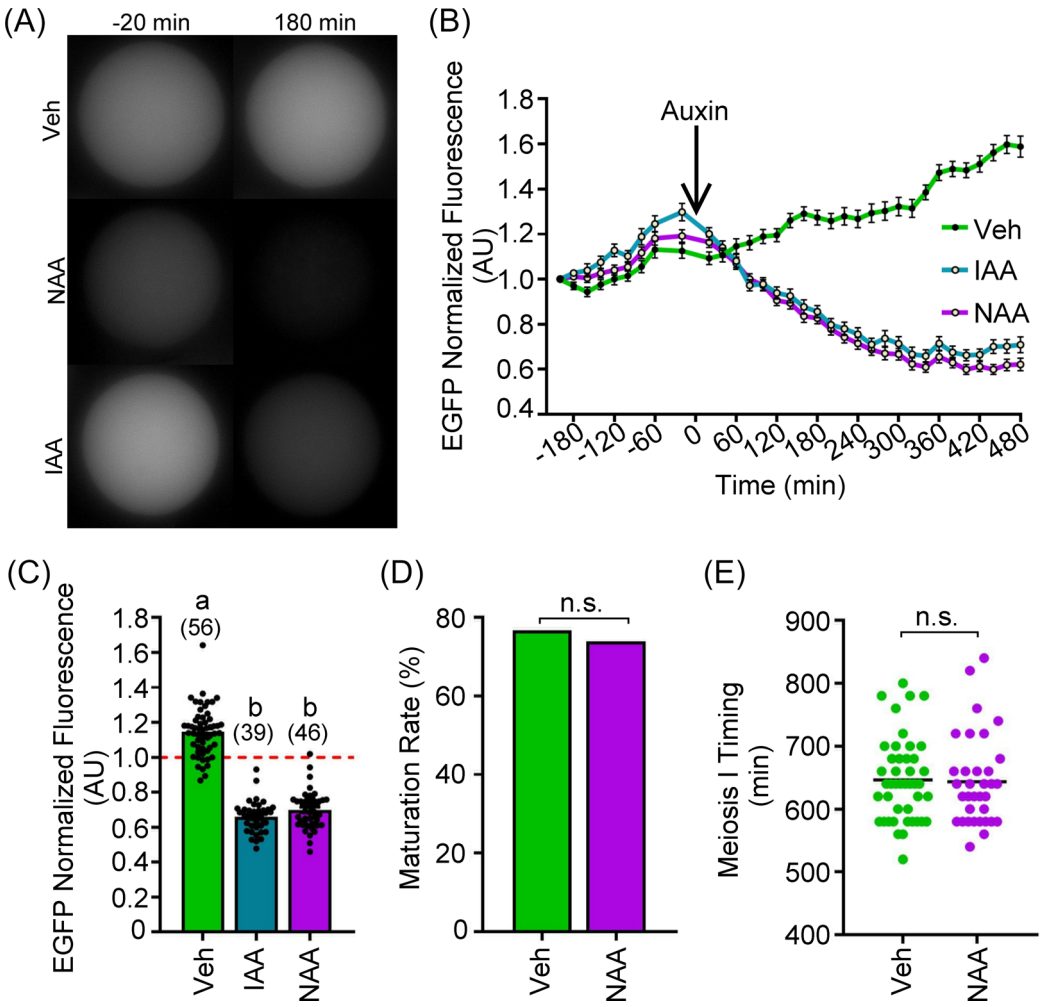

Figure 6. NAA induces auxin-inducible degradation to the same extent as IAA. Oocytes were injected with 0.4 μg/μl AIDm-EGFP cRNA and 2.0 μg/μl TIR1-myc cRNA, and allowed to express cRNA for 6 h prior to 500 μM IAA or NAA treatment. (A) Live-cell EGFP fluorescence (gray) in prophase I oocytes 20 min prior to (−20 min) and 180 min post IAA or NAA addition. (B) Graphical representation of EGFP fluorescence over time in vehicle, IAA, or NAA-exposed oocytes. Auxin was added at a concentration of 500 μM at t = 0 min (arrow). EGFP fluorescence normalized to expression at −180 min. (C) Graphical comparison of EGFP 180 min after auxin addition. EGFP fluorescence normalized to expression at −20 min (Kruskal–Wallis test with Dunn's post hoc). n = number of oocytes analyzed (39–46 over four technical replicates), $P < 0.0001$. (D, E) Graphical representation of percentage of oocytes at MII following 16 h of IVM and their time spent in meiosis I (D: Fisher's exact test; E: Mann-Whitney test). Bar graphs show mean, SEM, and individual oocyte scatter plot (C) or percentage of oocytes that emitted a first polar body (D). Line graph shows mean and SEM of EGFP fluorescence every 20 min. Scatter plot shows mean and individual oocyte meiosis I timing.

observed with continued NAA exposure (46.1 ± 4.2% EGFP loss with continuous NAA exposure; $P < 0.0001$). Although this increase in EGFP fluorescence was significant, AIDm-EGFP expression did not recover to the level observed in vehicle-only oocytes (Figures 8B, and Supplementary Figure S2A). Oocytes exposed to IAA, whether for the duration of the experiment (treatment 1 + 2) or for treatment 1 only (then vehicle for treatment 2), showed a small increase in EGFP fluorescence over the 500 min imaging (21.0 ± 6.1% EGFP recovery (IAA + Veh), $P = 0.0005$; 31.6 ± 8.8% EGFP recovery (IAA + IAA, i.e. continuous IAA), $P = 0.0077$). Of note, EGFP signal was distinctly different in oocytes continually exposed to IAA, with the fluorescence pattern being reminiscent of signals observed in oocytes just prior to death (Supplementary Figure 2B). This suggests that an increase in autofluorescence detected in the GFP channel could be occurring in these oocytes exposed to IAA for 24 h, and that the increase in fluorescence does not represent a true increase in AIDm-EGFP fluorescence. Importantly, oocytes treated with IAA continuously (IAA + IAA) had low survival compared to all other groups (12/33 oocytes survived (IAA + IAA) vs. 27/29 oocytes survived (IAA + Veh) vs. 31/32 oocytes survived (NAA + NAA) vs. 18/22 oocytes survived (NAA + Veh) vs. 19/26 oocytes survived (Veh + Veh) vs. 23/32 oocytes survived (Veh + IAA) oocytes survived). Note that only oocytes that survived the full 500 min of live-cell imaging were included in analysis.

Discussion

New methods to deplete proteins of interest are of increasing appeal, including for studies of meiosis in mammalian oocytes. Acute, specific, and temporally controllable protein removal is especially important in several instances: (a) when protein turnover is slow, limiting the utility of RNAi; (b) when proteins have essential roles

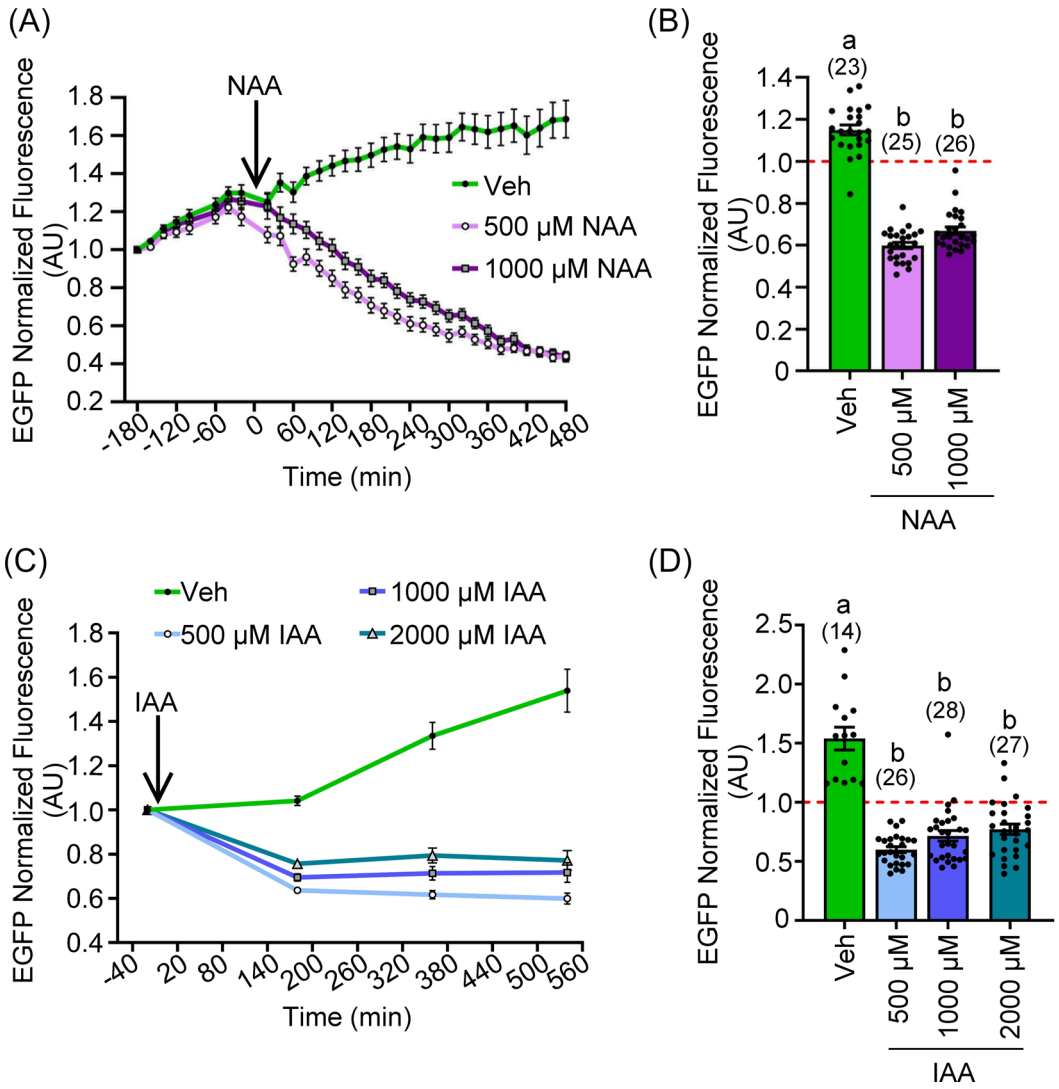

Figure 7. Increased auxin concentration has no impact on loss of exogenously expressed AIDm-EGFP. (A, B) Oocytes were injected with 0.4 μg/μl AIDm-EGFP cRNA and 2.0 μg/μl TIR1-myc cRNA, and allowed to express cRNA for 3 h prior to start of imaging. (A) Graphical representation of EGFP fluorescence over time in prophase I oocytes treated with vehicle, 500 μM, or 1000 μM NAA. NAA was added at 0 min (arrow). EGFP fluorescence normalized to expression at −180 min. (B) Graphical comparison of EGFP fluorescence before (−20 min) and after (180 min) NAA addition. EGFP fluorescence was normalized to expression at −20 min (Kruskal–Wallis test with Dunn's post hoc). n = number of oocytes analyzed (23–26 over three technical replicates), $P \leq 0.0001$. (C, D) Oocytes were injected with 0.4 μg/μl AIDm-EGFP cRNA and 2.0 μg/μl TIR1-myc cRNA, and allowed to express protein from the injected cRNA for 5 h prior to live-cell imaging. (C) Graphical representation of EGFP fluorescence over time in prophase I oocytes treated with vehicle, 500 μM, 1000 μM, or 2000 μM IAA. IAA was added at 0 min (arrow). EGFP fluorescence was normalized to expression at −20 min. (D) Graphical comparison of EGFP fluorescence before (−20 min) and after (180 min) IAA addition. EGFP fluorescence was normalized to expression at −20 min (Kruskal–Wallis test with Dunn's post hoc). n = number of oocytes analyzed (14–28 over two technical replicates), $P \leq 0.0001$. Line graphs show mean and SEM of EGFP fluorescence every 20 min (B) or 180 min (D). Bar graph shows mean, SEM, and individual oocyte scatter plot in auxin-exposed and control oocytes.

early in meiosis, thus prohibiting investigation of functions later in meiosis, and (c) when extended depletion leads to compensatory mechanisms or other events that confound data interpretation. Here we provide characterization of auxin-inducible degradation of an exogenously expressed protein in mouse oocytes, highlighting auxin-inducible degradation as a viable approach for rapid protein depletion at different stages of meiosis. This work also demonstrates the importance of auxin selection and TIR1 cRNA concentration for successful employment of auxin-inducible degradation in mammalian oocytes, extending the recent work that demonstrated that AID-tagged phospholipase Cζ could be degraded during egg activation [18].

We found that auxin-inducible degradation could be exploited during phases of meiotic arrest (prophase I and MII), and when oocytes where actively undergoing meiosis I (post-GVBD). Degradation kinetics were slightly slower than those observed in mammalian cell lines, and varied by meiotic stage, with the half-life of AIDm-EGFP in oocytes ranging from 41 min in MII-arrested oocytes to 107 min in prophase I-arrested oocytes treated with IAA. Cell line studies have found AID-tagged protein half-life to be 10–50 min in IAA- or NAA-treated cells, similar to what we observed in MII, but not prophase I or GVBD oocytes [13, 15, 25–28]. Additionally, addition of IAA to mouse embryos with endogenous AID-tagged proteins and a TIR1 transgene leads to complete loss of AID-tagged proteins

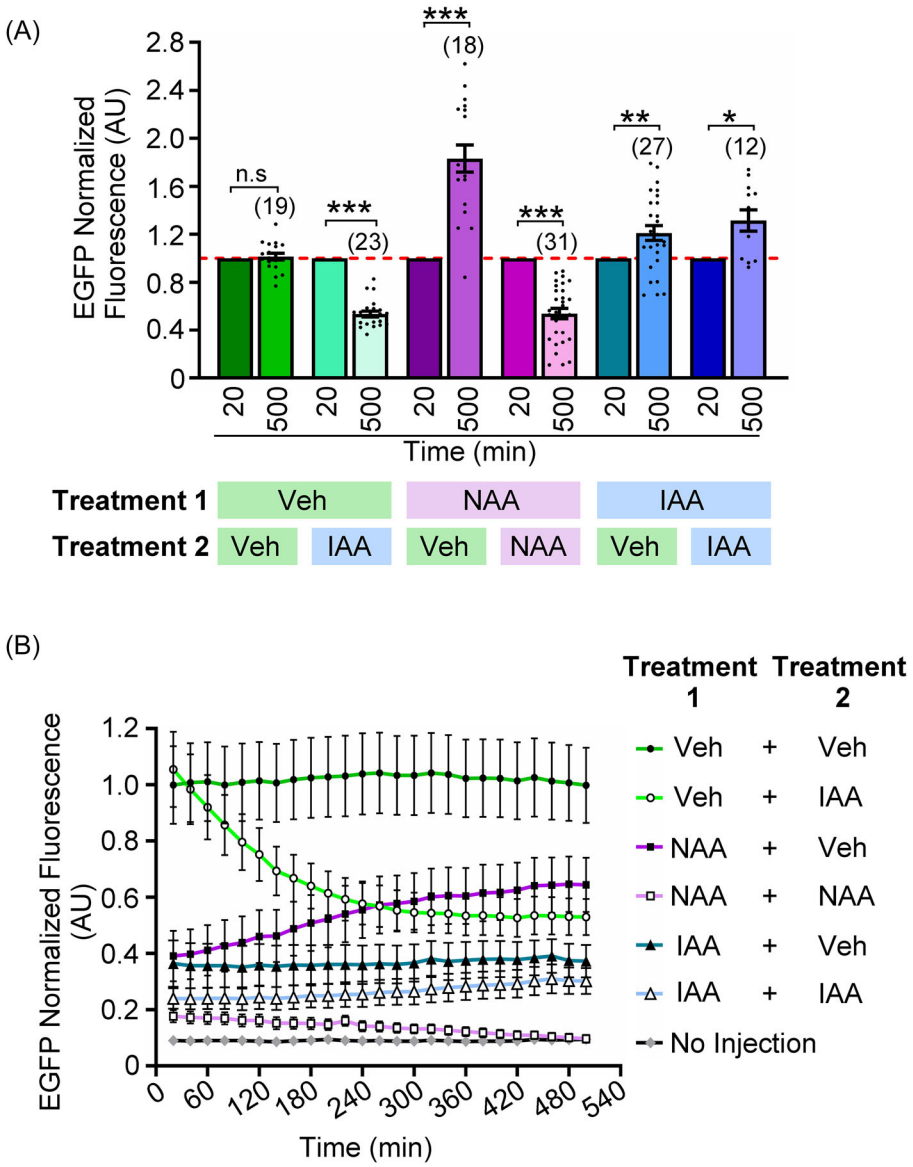

Figure 8. Auxin removal allows AIDm-EGFP expression to recover. Oocytes were injected with 0.4 μg/μl AIDm-EGFP cRNA and 2.0 μg/μl TIR1-myc cRNA, and allowed to express cRNA for 16 h in culture media containing vehicle, 500 μM IAA or 500 μM NAA. Just prior to imaging, oocytes were washed into media containing vehicle, 500 μM IAA, or 500 μM NAA. (A) Graphical comparison of EGFP fluorescence at the start of imaging (20 min) and 500 min later. Table shows culture conditions for the initial 16 h (treatment 1) and then culture conditions initiated immediately prior to live-cell imaging (treatment 2). EGFP fluorescence of each oocyte normalized to its expression at 20 min (ANOVA with Tukey's post hoc). n = number of oocytes analyzed (12–31 over three technical replicates); $^{***}P \leq 0.0001$, $^{**}P = 0.0005$, $^{*}P = 0.0077$. See the text and Supplementary Figure S2B for information on increased EGFP fluorescence in oocytes continually exposed to IAA. (B) Graphical representation of EGFP fluorescence over time. EGFP fluorescence normalized to average EGFP expression in oocytes continually exposed to vehicle at t = 20 min. Bar graph shows mean, SEM, and individual oocyte scatter plot. Line graphs show mean and SEM of EGFP fluorescence every 20 min.

in 30–80 min [29]. Of note, proteomic analysis of mouse oocytes has found that SKP1 and CUL1 protein expression increases ~20% and ~9%, respectively, between prophase I and MII arrest [30]. This increase in SCF protein subunits could account for the intensified degradation speed observed at MII arrest. We tested whether increasing auxin concentration would enhance the efficiency of auxin-inducible degradation in prophase I oocytes to the level seen in mitotic cells. However, raising auxin concentration failed to impact exogenous AIDm-EGFP degradation. While exogenous AIDm-EGFP had slow degradation kinetics in oocytes, there is significant protein-to-protein variability in auxin-inducible degradation. The Holland et al. study found half-lives of different proteins ranged from as little was 9 min to as long as 50 min [15]. It is therefore probable some proteins will undergo faster auxin-inducible degradation in oocytes. Furthermore, endogenous proteins, whose mRNA is under translational control of the oocyte, are likely to have improved auxin-inducible degradation. Nevertheless, the time frame for auxin-inducible degradation found for exogenously expressed AIDm-EGFP in oocytes is significantly shorter than the hours to days needed for RNAi-mediated

protein depletion, with time needed for RNA degradation and protein turnover.

We found that IAA-treated oocytes fail to progress through meiotic maturation during live-cell imaging with exposure to white light and 470 nm wavelength light. This agrees with a recent study in yeast showing that IAA treatment during live-cell imaging with 470 nm excitation of GFP produces growth defects [22]. The impaired yeast growth and oocyte maturation were not observed when the synthetic auxin NAA was used ([22] and our data here). IAA has been found to photodegrade into cytotoxins and free radicals [23, 24]. Importantly, IAA photodegradation can be eliminated with the use of yellow long-pass filters that remove UV, violet, and blue wavelengths [23]. In agreement with this, we found improved maturation rates in IAA-treated oocytes exposed to light outside the UV-to-blue spectrum. Interestingly, exposure of IAA-treated oocytes to 556 nm wavelength light only allowed partial oocyte maturation but 640 nm excitation had no impact on maturation rates. Since NAA-induced degradation can be slower for a subset of proteins [13, 22, 31, 32], use of fluorophores outside the UV-to-green wavelength spectrum, such as mCherry and mKate [33], could be valuable to avoid IAA-mediated cytotoxicity during live-cell imaging experiments.

Surprisingly, auxin type was also found to be an important factor in the reversibility of auxin-inducible degradation. Removal of NAA leads to robust recovery of exogenous AIDm-EGFP over 8 h. Conversely, IAA removal had only a modest impact on EGFP fluorescence intensity. To our knowledge, this is the first-time distinct recovery patterns have been observed when different auxins have been employed. In experiments in which reversibility is desirable, NAA should be considered as the auxin of choice, as NAA induces similar degradation as IAA, but proteins removed by NAA-induced degradation have improved recovery ability. The slow recovery of exogenous AIDm-EGFP after removal of auxin was not unexpected. In our study and others', removal of auxin allowed a slow recovery of the protein of interest over a period of hours to $\geq$50% of the starting protein level [22, 32, 34]. This gradual re-accumulation of protein is due to protein translation being a generally slower process than proteasome-mediated degradation.

In recent years, there has been a growing number of approaches developed to directly deplete proteins of interest. These methods have advantages over gene knockout and RNAi/morpholino-mediated knockdown, which are chronic in nature and rely on protein turnover. Two recent developments in this area include auxin-inducible degradation and the novel antibody-based Trim-Away, with both having distinct advantages and limitations [11, 13]. Notably, Trim-Away eliminates the need to create animal models containing modified endogenous proteins, as would be required with many applications of auxin-inducible degradation, and Trim-Away is ~2- to 12-fold faster. Auxin-inducible degradation has different advantages as compared to Trim-Away. The first advantage is the ability to mediate protein loss throughout meiosis with the simple addition of auxin to culture media. Trim-Away, on the other hand, begins to deplete proteins following introduction of the antibody to the protein of interest, and therefore relies on microinjection at different stages of meiosis to induce protein loss. Additionally, Trim-Away is dependent on antibodies. This can be an advantage when genetic engineering is not feasible, such as with human oocytes. However, the availability and specificity of antibodies likely affect the effectiveness of Trim-Away. During the preparation of this manuscript, a system that utilized AID-tagged nanobodies to deplete endogenous proteins in cell lines and zebrafish was developed [25]. This nanobody-based auxin-inducible degradation provides a valuable approach that is in the middle ground between Trim-Away's ability to deplete unmodified proteins and the temporal ease of auxin-inducible protein degradation, which could be particularly useful in human oocytes or animal models in which genetic engineering is not practical. The development of CRISPR/Cas9 will significantly streamline the genetic engineering needed for the use of auxin-inducible degradation of endogenous proteins in murine model systems. Of note, CRISPR/Cas9 was recently used to AID-tag endogenous *Sox2*, *Gata6*, and *Nanog*, and to express a TIR1 transgene under the actin β promoter in mouse embryos [29]. A different application of this auxin-inducible degradation method is the removal of exogenously expressed proteins, as described here, which can be used for manipulation of molecules and pathways of interest using phosphomimic, dominant-negative, or constitutively active variants [9, 35–40]. The addition of an AID tag to exogenously expressed proteins allows for further manipulation in oocytes during progression through meiosis.

Another consideration is the reversibility of auxin-inducible degradation. Gene knockout, RNAi, and Trim-Away lead to the permanent loss of endogenous proteins of interest in oocytes [11]. The reversibility of auxin-inducible degradation is an advantage, although with a caveat. For proteins for which only a small amount is needed in oocytes, the gradual recovery will be sufficient to rescue phenotype. However, for proteins that are required at high concentrations, auxin-inducible degradation could be viewed as relatively permanent, comparable to Trim-Away, RNAi, and gene knockout. If reversibility is essential, use of a protein caging methods, such as the recently developed auxin-mediated proximity control system, should be considered [41].

In summary, this study provides detailed evaluation of the efficiency of auxin-inducible protein degradation in mammalian oocytes. We show for the first time that this method of protein depletion can be used on exogenously expressed proteins throughout meiosis. Additionally, we highlight important considerations for experimental design, including TIR1 concentration and type of auxin employed.

Supplementary data

Supplementary data are available at *BIOLRE* online.

Supplementary Figure S1: Removal of oocyte EGFP autofluorescence decreases EGFP normalized fluorescence in auxin-treated oocytes. Graphical representation of EGFP fluorescence over time in vehicle, IAA, CHX, or IAA and CHX-treated oocytes with and without autofluorescence adjustment. Auxin was added at a concentration of 500 μM at t = 0 min (arrow). EGFP fluorescence normalized to expression at t = −180 min. Line graph shows mean and SEM of EGFP fluorescence every 20 min.

Supplementary Figure S2: EGFP recovery normalized to vehicle control oocytes and comparison of continuously exposed auxin vs. auxin washout oocytes at 500 min. (A) Graphical comparison of EGFP fluorescence at the start of imaging (20 min) and 500 min later. Table shows the treatment that oocytes were subjected to for 16 h prior to imaging (treatment 1; no auxin [vehicle] or NAA or IAA) and then at the start of imaging (treatment 2). EGFP fluorescence normalized to average EGFP expression in oocytes continually exposed to vehicle at t = 20 min. (B) Live-cell excitation of oocytes at 470 nm in oocytes continuously exposed to IAA and oocytes washed out of IAA into vehicle-containing medium prior to imaging. Oocytes continually exposed to IAA showed an increase in fluorescence with a

pattern distantly different for oocytes in vehicle-containing medium. This pattern likely reflects an increase in autofluorescence in sick and dying oocytes.

Supplementary Table S1: Cloning primers and plasmid constructs.

Acknowledgments

The authors greatly acknowledge the plasmids provided by Dr Andrew Holland (Johns Hopkins University) and Dr Carmen Williams (National Institute of Environmental Health Sciences). We also thank Dr Christine Lee (Johns Hopkins University) for assistance with live-cell imaging.

Authors' contributions

NJC contributed to the design of the study, performed data acquisition, data analysis/interpretation, and was responsible for drafting and revising the manuscript. JPE contributed to the conception and design of the study, data interpretation, and revising the manuscript. Both authors reviewed and approved the final manuscript.

Conflict of interest

The authors declare no conflict of interest.

References

1. Toyama Brandon H, Savas Jeffrey N, Park Sung K, Harris Michael S, Ingolia Nicholas T, Yates John R, III, Hetzer Martin W. Identification of long-lived proteins reveals exceptional stability of essential cellular structures. *Cell* 2013; **154**:971–982.
2. Smoak EM, Stein P, Schultz RM, Lampson MA, Black BE. Long-term retention of CENP-A nucleosomes in mammalian oocytes underpins transgenerational inheritance of centromere identity. *Curr Biol* 2016; **26**:1110–1116.
3. Li J, Tang J-X, Cheng J-M, Hu B, Wang Y-Q, Aalia B, Li X-Y, Jin C, Wang X-X, Deng S-L, Zhang Y, Chen S-R et al. Cyclin B2 can compensate for Cyclin B1 in oocyte meiosis I. *J Cell Biol* 2018; **217**(11):3901–3911.
4. Luo J, McGinnis LK, Kinsey WH. Role of Fyn kinase in oocyte developmental potential. *Reprod Fertil Dev* 2010; **22**:3901–3911.
5. Adhikari D, Diril MK, Busayavalasa K, Risal S, Nakagawa S, Lindkvist R, Shen Y, Coppola V, Tessarollo L, Kudo NR, Kaldis P, Liu K. Mastl is required for timely activation of APC/C in meiosis I and Cdk1 reactivation in meiosis II. *J Cell Biol* 2014; **206**:843–853.
6. Zhao X, Yu D, Feng C, Deng X, Wu D, Jin M, Wang E, Wang X, Yu B. Role of Greatwall kinase in release of mouse oocytes from diplotene arrest. *Develop Growth Differ* 2014; **56**:669–678.
7. Li Y-H, Kang H, Xu Y-N, Heo Y-T, Cui X-S, Kim N-H, Oh JS. Greatwall kinase is required for meiotic maturation in porcine oocytes. *Biol Reprod* 2013; **89**:53.
8. Homer H, Gui L, Carroll J. A spindle assembly checkpoint protein functions in prophase I arrest and prometaphase progression. *Science* 2009; **326**:991–994.
9. Liang X-W, Zhang Q-H, Li M, Yuan J, Li S, Sun S-C, Ouyang Y-C, Schatten H, Sun Q-Y. BubR1 is a spindle assembly checkpoint protein regulating meiotic cell cycle progression of mouse oocyte. *Cell Cycle* 2010; **9**:1112–1121.
10. Touati SA, Buffin E, Cladiere D, Hached K, Rachez C, van Deursen JM, Wassmann K. Mouse oocytes depend on BubR1 for proper chromosome segregation but not for prophase I arrest. *Nat Commun* 2015; **6**:6946.
11. Clift D, McEwan WA, Labzin LI, Konieczny V, Mogessie B, James LC, Schuh M. A method for the acute and rapid degradation of endogenous proteins. *Cell* 2017; **171**:1692–1706.e18.e1618.
12. Willems AR, Schwab M, Tyers M. A hitchhiker's guide to the cullin ubiquitin ligases: SCF and its kin. *Biochim Biophys Acta* 2004; **1695**:133–170.
13. Nishimura K, Fukagawa T, Takisawa H, Kakimoto T, Kanemaki M. An auxin-based degron system for the rapid depletion of proteins in nonplant cells. *Nat Methods* 2009; **6**:917–922.
14. Kanke M, Nishimura K, Kanemaki M, Kakimoto T, Takahashi TS, Nakagawa T, Masukata H. Auxin-inducible protein depletion system in fission yeast. *BMC Cell Biol* 2011; **12**:8.
15. Holland AJ, Fachinetti D, Han JS, Cleveland DW. Inducible, reversible system for the rapid and complete degradation of proteins in mammalian cells. *Proc Natl Acad Sci USA* 2012; **109**:E3350–E3357.
16. Lambrus BG, Moyer TC, Holland AJ. Applying the auxin-inducible degradation system for rapid protein depletion in mammalian cells. In: Maiato H, Schuh M (eds.), *Methods in Cell Biology*, vol. 144. Amsterdam, New York, Oxford: Academic Press; 2018:107–135.
17. Gray WM, del Pozo JC, Walker L, Hobbie L, Risseeuw E, Banks T, Crosby WL, Yang M, Ma H, Estelle M. Identification of an SCF ubiquitin-ligase complex required for auxin response in Arabidopsis thaliana. *Genes Dev* 1999; **13**:1678–1691.
18. Miura K, Matoba S, Ogonuki N, Namiki T, Ito J, Kashiwazaki N, Ogura A. Application of auxin-inducible degron technology to mouse oocyte activation with PLCζ. *J Reprod Dev* 2018; **64**:319–326.
19. Matthews LM, Evans JP. α-endosulfine (ENSA) regulates exit from prophase I arrest in mouse oocytes. *Cell Cycle* 2014; **13**:1639–1649.
20. Schindelin J, Arganda-Carreras I, Frise E, Kaynig V, Longair M, Pietzsch T, Preibisch S, Rueden C, Saalfeld S, Schmid B, Tinevez J-Y, White DJ et al. Fiji: an open-source platform for biological-image analysis. *Nat Methods* 2012; **9**:676–682.
21. Camlin NJ, McLaughlin EA, Holt JE. Kif4 is essential for mouse oocyte meiosis. *PLoS One* 2017; **12**:e0170650.
22. Papagiannakis A, de Jonge JJ, Zhang Z, Heinemann M. Quantitative characterization of the auxin-inducible degron: a guide for dynamic protein depletion in single yeast cells. *Sci Rep* 2017; **7**:4704.
23. Stasinopoulos TC, Hangarter RP. Preventing photochemistry in culture media by long-pass light filters alters growth of cultured tissues. *Plant Physiol* 1990; **93**:1365–1369.
24. Folkes LK, Wardman P. Enhancing the efficacy of photodynamic cancer therapy by radicals from plant auxin (indole-3-acetic acid). *Cancer Res* 2003; **63**:776.
25. Daniel K, Icha J, Horenburg C, Müller D, Norden C, Mansfeld J. Conditional control of fluorescent protein degradation by an auxin-dependent nanobody. *Nat Commun* 2018; **9**:3297.
26. Nora EP, Goloborodko A, Valton A-L, Gibcus JH, Uebersohn A, Abdennur N, Dekker J, Mirny LA, Bruneau BG. Targeted degradation of CTCF decouples local insulation of chromosome domains from genomic compartmentalization. *Cell* 2017; **169**:930–944.e22 e922.
27. Natsume T, Kiyomitsu T, Saga Y, Kanemaki MT. Rapid protein depletion in human cells by auxin-inducible degron tagging with short homology donors. *Cell Rep* 2016; **15**:210–218.
28. Lambrus BG, Uetake Y, Clutario KM, Daggubati V, Snyder M, Sluder G, Holland AJ. p53 protects against genome instability following centriole duplication failure. *J Cell Biol* 2015; **210**:63–77.
29. Gu B, Posfai E, Rossant J. Efficient generation of targeted large insertions by microinjection into two-cell-stage mouse embryos. *Nat Biotechnol* 2018; **36**:632–637.
30. Wang S, Kou Z, Jing Z, Zhang Y, Guo X, Dong M, Wilmut I, Gao S. Proteome of mouse oocytes at different developmental stages. *Proc Natl Acad Sci USA* 2010; **107**:17639–17644.
31. Kreidenweiss A, Hopkins AV, Mordmüller B. 2A and the auxin-based degron system facilitate control of protein levels in plasmodium falciparum. *PLoS One* 2013; **8**:e78661.
32. Farr CJ, Antoniou-Kourounioti M, Mimmack ML, Volkov A, Porter ACG. The α isoform of topoisomerase II is required for hypercompaction of mitotic chromosomes in human cells. *Nucleic Acids Res* 2014; **42**:4414–4426.
33. Rodriguez EA, Campbell RE, Lin JY, Lin MZ, Miyawaki A, Palmer AE, Shu X, Zhang J, Tsien RY. The growing and glowing toolbox of fluorescent and photoactive proteins. *Trends Biochem Sci* 2017; **42**:111–129.

34. Zhang L, Ward JD, Cheng Z, Dernburg AF. The auxin-inducible degradation (AID) system enables versatile conditional protein depletion in C. elegans. *Development* 2015; **142**:4374–4384.
35. Nguyen AL, Marin D, Zhou A, Gentilello AS, Smoak EM, Cao Z, Fedick A, Wang Y, Taylor D, Scott JRT, Xing J, Treff N et al. Identification and characterization of Aurora kinase B and C variants associated with maternal aneuploidy. *Mol Hum Reprod* 2017; **23**:406–416.
36. Jansova D, Koncicka M, Tetkova A, Cerna R, Malik R, del Llano E, Kubelka M, Susor A. Regulation of 4E-BP1 activity in the mammalian oocyte. *Cell Cycle* 2017; **16**:927–939.
37. Feng R, Sang Q, Kuang Y, Sun X, Yan Z, Zhang S, Shi J, Tian G, Luchniak A, Fukuda Y, Li B, Yu M et al. Mutations in TUBB8 cause human oocyte meiotic arrest. *N Engl J Med* 2016; **374**:223–232.
38. Larson SM, Lee HJ, Hung P-h, Matthews LM, Robinson DN, Evans JP. Cortical mechanics and meiosis II completion in mammalian oocytes are mediated by myosin-II and Ezrin-Radixin-Moesin (ERM) proteins. *Mol Biol Cell* 2010; **21**:3182–3192.
39. Gardner AJ, Knott JG, Jones KT, Evans JP. CaMKII can participate in but is not sufficient for the establishment of the membrane block to polyspermy in mouse eggs. *J Cell Physiol* 2007; **212**:275–280.
40. Chen J, Hudson E, Chi MM, Chang AS, Moley KH, Hardie DG, Downs SM. AMPK regulation of mouse oocyte meiotic resumption in vitro. *Dev Biol* 2006; **291**:227–238.
41. Zhao W, Nguyen H, Zeng G, Gao D, Yan H, Liang F-S. A chemically induced proximity system engineered from the plant auxin signaling pathway. *Chem Sci* 2018; **9**:5822–5827.